

Title: Vitamin D regulation of a SOD1-to-SOD2 antioxidative switch to prevent osteosarcoma transformation

Author: Thomas S. Lisse<sup>1,2\*</sup>

Affiliations: <sup>1</sup>University of Miami, Biology Department  
1301 Memorial Drive, Cox Science Center, Coral Gables, Florida 33146 USA.

<sup>2</sup>Sylvester Comprehensive Cancer Center, Miller School of Medicine, University of Miami, Miami, Florida 33136 USA.

\*Correspondence:

Thomas Lisse Ph.D.  
Department of Biology, The University of Miami  
tom.lisse@miami.edu  
305-284-3957

Keywords: Osteosarcoma, cancer, tumor, vitamin D, vitamin D deficiency, vitamin D receptor, VDR, ROS, mitochondria, MG-63, SOD, SOD1, SOD2, stress

Competing interests: Authors have nothing to declare.

Funding: Supported by start-up funds from the College of Arts and Sciences, Biology Department, University of Miami, Coral Gables, Florida

Supported by Grant # IRG-17-183-16 from the American Cancer Society, and from the Sylvester Comprehensive Cancer Center at the Miller School of Medicine, University of Miami

## Abstract

Superoxide, a form of reactive oxygen species (ROS), is catabolized by superoxide dismutase (SOD) and contributes to carcinogenesis via the oxidative damage it inflicts on cells. The aim of this research was to analyze the potential vitamin D-mediated regulation of the antioxidative “SOD1-to-SOD2 switch” within the human MG-63 osteosarcoma model. For this study, real-time PCR analysis was performed using MG-63 cells exposed to metabolically active 1,25(OH)<sub>2</sub>D<sub>3</sub>. First, a sustained statistically significant >2-fold suppression of proliferating cell nuclear antigen (PCNA) transcripts was observed after 10nM but not at 100nM of 1,25(OH)<sub>2</sub>D<sub>3</sub> treatment, suggesting a cytostatic effect. In order to assess regulators of mitochondrial oxidative phosphorylation, gene expression of *COX2* and *COX4I1* of the mitochondrial complex IV and antioxidative enzymes (*SOD1*, *SOD2* and *Catalase (CAT)*) were monitored. For *COX2* and *COX4I1*, no changes in gene expression were observed. However, a concomitant decrease in *CAT* and *SOD1* mRNA, and increase in *SOD2* mRNA after 24 hours of 10nM 1,25(OH)<sub>2</sub>D<sub>3</sub> treatment were observed. A ~8-fold increase in *SOD2* mRNA was apparent after 48 hours. The significant increase in *SOD2* activity in the presence of vitamin D indicates an antioxidant potential and sensitization of vitamin D during osteosarcoma transformation and mitochondrial detoxification over time.

## Introduction

Vitamin D is a steroid hormone produced in the skin, or obtained in varying quantities through dietary or supplementary means<sup>1</sup>. Vitamin D is metabolized through two subsequent hydroxylation steps, resulting in its metabolically active form, 1,25(OH)<sub>2</sub>D<sub>3</sub> (also known as calcitriol or 1,25D<sub>3</sub>). 1,25D<sub>3</sub> exerts its genomic effects by binding to the vitamin D receptor (VDR), a member of the nuclear receptor super family<sup>2-13</sup>. It has long been recognized that vitamin D has noncalcemic functions in controlling the cell cycle, differentiation and apoptosis, and its analogues are used in cancer prevention and treatment<sup>14,15</sup>. Understanding how vitamin D can regulate these processes is central to applications toward specialized cancer treatment<sup>15</sup>.

It is widely accepted that oxidative damage is one among several key factors that limits lifespan. Superoxide (O<sub>2</sub><sup>-</sup>) anions are produced as a free radical reactive oxygen species (ROS) by-product of oxygen metabolism and mitochondrial respiration, and can damage cells at high concentrations if left unchecked<sup>16</sup>. Superoxide anions are produced and accumulate in the matrix and the intermembrane space of the mitochondria, and are also produced from the enzymes NOX/DUOX localized at the plasma membrane<sup>17</sup>. Excessive superoxide in the cell results in damage to mitochondrial DNA, proteins and lipids, and ultimately leads to irreversible damage to organelles. To counter the effects of elevated superoxide anions, cells express superoxide-scavenging enzymes superoxide dismutase (SOD)<sup>18</sup>. SOD catalyzes the disproportionation of superoxide into either molecular oxygen or hydrogen peroxide as part of its antioxidant defense mechanism. Hence, SOD enzymes maintain a range of ROS in order to control potential toxicity, as well as downstream cellular and signaling functions<sup>19</sup>. There are three forms of SODs, and the localization of the SODs reflect their antioxidative roles within cells. SOD1 is mostly sequestered in the cytosol but can also localize to the mitochondria, SOD2 in the matrix of mitochondria<sup>20</sup>, and SOD3 is in the extracellular space<sup>18</sup>. Several regulators of SODs have been characterized. For example, SOD2 is regulated by SIRT3-mediated deacetylation that can attenuate excessive production of mitochondrial ROS under disease conditions<sup>21</sup>.

Vitamin D is known to exert its anti-cancer effects by a variety of mechanisms, most prominently studied is through G<sub>1</sub> cell cycle arrest<sup>7,10,22-24</sup>. However, there are several studies that have looked at the role of vitamin D on ROS production and detoxification. For example, a recent paper has shown that supraphysiological levels of calcitriol exerts its anti-tumor effects in a

mouse cell model of osteosarcoma via induction of the endoplasmic reticulum stress response with a concomitant increase in intracellular ROS<sup>25</sup>. In addition, cDNA microarray analysis using human prostate epithelial cells revealed that calcitriol (50nM) can promote SOD2 expression (2.01 fold increase, 24 hours)<sup>26</sup>, as well as the early expression of the antioxidant thioredoxin reductase 1 (TXNRD1; 2.8 fold increase, 6 hours)<sup>27</sup>. Another cDNA microarray study using androgen-sensitive prostate cancer cells identified a 2.6 fold increase in SOD1 at 10nM of 1,25D<sub>3</sub> treatment for 24 hours<sup>27</sup>. Calcitriol was also found to induce glucose-6-phosphate dehydrogenase (G6PD) transcription in a VDR-dependent manner within non-malignant prostate cancer cells to maintain NADPH levels for the production the ROS scavenger glutathione<sup>28</sup>. To compliment these studies, the aim of this research was to analyze the potential vitamin D-mediated regulation of the “SOD1-to-SOD2 switch” within the MG-63 p53-independent osteosarcoma model that was recently characterized between non-tumorigenic and tumorigenic breast cancer cells<sup>29</sup>.

## Results

### Effects of 1,25D<sub>3</sub> on MG-63 osteosarcoma cell viability using the MTT assay

In order to establish the *in vitro* conditions to investigate the mechanism of action toward mitochondrial dynamics, MG-63 cellular response to a 10-fold serial dilution of 1,25D<sub>3</sub> was assessed using the 3-[4,5-dimethylthiazol-2-yl]-2,5 diphenyl tetrazolium bromide (MTT) assay (**Figure 1**). MG-63 cells were treated with 1,25D<sub>3</sub> at concentrations ranging from 1pM to 1μM, and cell viability was assessed at 24 and 48 hours post treatment. In addition, two different media conditions were compared to access the synergistic effects of liganded VDR signaling. For one, a charcoal-stripped fetal bovine serum (FBS)-based media was applied to assess the singular role of VDR signaling within MG-63 osteosarcoma cells. For the other, a standard complete media with normal FBS was applied to study the synergistic effects of VDR signaling with other hormone ligands in the system. Interestingly, when cultured with charcoal-stripped media, 1,25D<sub>3</sub> was unable to inhibit viability of MG-63 cells even at the highest concentration of 1μM for both 24 and 48 hours after treatment (**Figure 1A**). However, in complete media a mild suppression of cell viability was observed only after 24 hours of 1,25D<sub>3</sub> treatment at the higher concentration range of 10-1000nM ( $p < 0.05-0.001$ ) (**Figure 1A**). This suppression in cell viability became even more pronounced after 48 hours of 1,25D<sub>3</sub> treatment within the lower 0.1-1000nM

range (**Figure 1A**;  $p < 0.05-0.001$ ). Based on these studies, it appears that 1,25D<sub>3</sub> treatment over time has a significant suppressive effect on MG-63 cell viability within human serum levels down to the pmol/L range<sup>30</sup>.

Based on our dose curve for MG-63 cells, the IC<sub>50</sub> value (i.e. the concentration that provides a response halfway between the maximal and the minimally inhibited response) for 1,25D<sub>3</sub> was determined (**Figure 1A**). The 1,25D<sub>3</sub> concentrations were transformed to log value, whereby the model assumes that the response curve has a standard slope equal to a Hill slope (or slope factor) of -1.0. As there were no maximal response for the 24-hour complete media and 24/48-hour charcoal-stripped media treated samples, the IC<sub>50</sub> values could not be determined in these cases. For the 48-hour complete media condition, the best-fit IC<sub>50</sub> value based on non-linear regression was 55.43nM ( $\log IC_{50} = 1.74$ ), whereby the goodness of fit R<sup>2</sup> value was 0.8773, and correlated with the transformed % inhibition data (**Figure 1C**). In order to study the involvement and regulatory mechanisms of 1,25D<sub>3</sub> on mitochondrial dynamics, 10nM and 100nM concentrations were further investigated which encapsulates the determined IC<sub>50</sub> value.

### **Characterization of 1,25D<sub>3</sub>-mediated cell cycle and vitamin D catabolic and osteogenic genes in MG-63 osteosarcoma cells**

To acquire further insight into the molecular mechanisms underlying the increased inhibition of MG-63 osteosarcoma cell viability by 1,25D<sub>3</sub>, gene expression analysis was performed of cell cycle, vitamin D signaling and osteogenic-related genes. For this part, MG-63 cells were treated with 10nM and 100nM 1,25D<sub>3</sub>, or vehicle (equi-volume ethanol) for 24 and 48 hours in complete media. First, proliferating cell nuclear antigen (PCNA) mRNA was appraised by real-time PCR to assess the level of DNA replication in the samples. After 1,25D<sub>3</sub> treatment at 10nM, a statistically significant >2-fold suppression of PCNA transcripts was observed compared to vehicle-treated samples for both the 24- and 48-hour time points (**Figure 2A**). However, no large difference in PCNA transcript levels was observed at the higher 100nM of 1,25D<sub>3</sub> at both time points, which was also confirmed upon vitamin D antagonist ZK159222 (VAZ) treatment that blocks VDR genomic actions<sup>31</sup> (**Figure 2A**). These results suggest that 1,25D<sub>3</sub> suppresses DNA replication (i.e. cell division) only at 10nM in the system.

In order to monitor the control of vitamin D signaling, cytochrome P450 family 24 subfamily A member 1 (CYP24A1) and VDR transcript levels were monitored. CYP24A1 is a vitamin D<sub>3</sub> 24-

hydroxylase and a VDR target gene that is involved in the catabolism of calcitriol. After treatment of MG-63 cells with 10nM 1,25D<sub>3</sub> for both 24 and 48 hours, there was a significant reduction in the level of CYP24A1 compared to vehicle-treated controls (**Figure 2B**). However, after 100nM 1,25D<sub>3</sub> treatment, there was a significant increase in CYP24A1 mRNA compared to 10nM-treated samples. This response was mediated by genomic VDR signaling, as a significant decrease in CYP24A1 mRNA was observed after VAZ co-treatment. This observation suggests a vitamin D-dependency at the 100nM concentration, and an overall suppression of vitamin D signaling through 1,25D<sub>3</sub> catabolism. VDR mRNA level was measured and shown to be significantly decreased after 10nM 1,25D<sub>3</sub> treatment that was more striking after 48 hours (**Figure 2C**). However, there was no change in VDR mRNA levels after 100nM 1,25D<sub>3</sub> treatment at both time points. Furthermore, the VDR mRNA level was not altered after VAZ treatment confirming the presence of receptor in the system and limited autoregulation<sup>7</sup>. Although CYP24A1 is commonly upregulated in cancers and thought to be one mode for vitamin D resistance<sup>32</sup>, this appears not to be the case for MG-63 cells treated with 100nM 1,25D<sub>3</sub> based on the MTT results (**Figure 1A**). This suggests other anti-cancer strategies upon high levels of vitamin D, including apoptosis<sup>33</sup> and/or induction of other stress pathways such as those involving the endoplasmic reticulum<sup>25</sup>.

In addition, osteocalcin (encoded by *BGLAP*) mRNA levels were monitored. Osteocalcin is a secreted non-collagenous protein hormone often used to assess osteoblast activity, which is under direct VDR regulation<sup>34</sup>. At 10nM 1,25D<sub>3</sub> treatment for both 24 and 48 hours, a significant and drastic decrease in BGLAP mRNA levels was observed (**Figure 2D**). However, an increase to near baseline levels of BGLAP mRNA was observed after 100nM 1,25D<sub>3</sub> treatment, which was abrogated upon VAZ treatment confirming VDR dependency. As increased osteocalcin production is known to cause endoplasmic reticulum stress coupled with elevated oxygen consumption<sup>35</sup>, the differences between 10nM and 100nM 1,25D<sub>3</sub> may further represent a switch from cytostatic to cytotoxic metabolism, respectively.

### **Vitamin D treatment does not inhibit the transcription of respiratory chain genes *COXII* and *COX4I1* in MG-63 cells**

Recent studies have shown that vitamin D can suppress the production of cellular ROS in MG-63 cells<sup>25</sup>, however the mode of action is unknown. First mitochondrial and nuclear transcription of cytochrome c oxidase subunit 2 (COXII) and subunit 4 isoform 1 (COX4I1) mRNA,

respectively, were characterized after 1,25D<sub>3</sub> treatment over time as potential players in ROS regulation. These proteins are subunits of cytochrome c oxidase complex IV part of the active mitochondrial respiratory chain and contribute to the proton electrochemical gradient across the inner mitochondrial membrane. Previous studies have shown that both of these subunits were inhibited after 1,25D<sub>3</sub> treatment in skin keratinocyte models<sup>36</sup>, and may be involved in osteosarcoma. However, after both 10nM and 100nM 1,25D<sub>3</sub> and VAZ co-treatments of MG-63 cells for 24 and 48 hours, no striking differences in the gene expression of both *COXII* and *COX4I1* were observed (**Figure 3A,B**). These results suggest that 1,25D<sub>3</sub> does not modulate active cytochrome c oxidase via COXII and COX4I1 subunits at the transcriptional level. These results point to alternative mitochondrial regulators, including perhaps other components of the electron transport chain, in the regulation of ROS by vitamin D<sup>25</sup>.

### **SOD1-to-SOD2 antioxidative switch after vitamin D treatment of MG-63 osteosarcoma cells**

Given the known increase in ROS among MG-63 osteosarcoma cells<sup>25</sup>, it was hypothesized that antioxidant defense mechanisms may be involved in vitamin D-dependent suppression of ROS production. Specific SOD activities are correlated with tumorigenicity<sup>16,29</sup>, therefore the transcription of the SOD genes within 1,25D<sub>3</sub>-treated MG-63 cells was monitored over time. A significant and dramatic decrease in the level of SOD1 transcript was observed only after 24 and 48 hours of 10nM 1,25D<sub>3</sub> treatment (**Figure 3C**). At 100nM of 1,25D<sub>3</sub> there was no change in SOD1 levels with or without VAZ, suggesting no direct VDR-dependent regulatory role at higher concentrations of ligand. Interestingly, a dramatic >2.5-8-fold time-dependent persistent increase in SOD2 mRNA levels was observed only with the lower 10nM 1,25D<sub>3</sub> concentration at both time points (**Figure 3D**). Once again, at the higher 100nM 1,25D<sub>3</sub> concentration the regulatory role of VDR toward SOD2 activity was abrogated. Catalase is a peroxisomal enzyme that rapidly degrades hydrogen peroxide (H<sub>2</sub>O<sub>2</sub>) to O<sub>2</sub> and H<sub>2</sub>O. As SODs may yield H<sub>2</sub>O<sub>2</sub>, the mRNA levels of the H<sub>2</sub>O<sub>2</sub> antioxidant catalase (CAT) were monitored, and a moderate and statistically significant decrease was observed only after 10nM 1,25D<sub>3</sub> treatment at the 24-hour time point (**Figure 3E**). However, a steady increase following another 24 hours back toward baseline was also observed (**Figure 3E**). This suggests the protective role of vitamin D treatment relying less on CAT antioxidant production during the early stages of treatment, and the potential decrease in H<sub>2</sub>O<sub>2</sub> efflux from the mitochondria. Lastly, the real-time PCR results were arranged using arbitrary units in order to compare amounts of transcripts across

experiments. In this way, it became more evident that after 1,25D<sub>3</sub> treatment there was a clear shift from SOD1 to SOD2 initiated at the 24-hour time point (**Figure 3F**). However, by the 48-hour time point SOD2 levels exceeded SOD1 levels to complete the “switch” (**Figure 3F**). The switch from SOD1 to SOD2 may signify the importance of the cellular distribution and actions of each SOD enzyme, cytosol versus mitochondria, respectively. Overall, these findings suggest an active time and concentration-dependent mitochondrial reparative process involving specific SOD enzymes engaged after vitamin D treatment within MG-63 osteosarcoma cells as part of vitamin D's anti-cancer effects (**Figure 4**).

## Discussion

The major finding of this paper is that MG-63 osteosarcoma cells can respond to adaptive signals such as vitamin D to suppress the transformation process by upregulation of SOD2. The degree to which the vitamin D-SOD network offers specific cytoprotective and antioxidative effects is unclear, and the focus of future studies. Importantly, this form of regulation is tightly controlled in a 1,25D<sub>3</sub> concentration and time dependent manner which argues for maintenance of proper vitamin D levels in the body. The importance of SODs are reflected in mice either lacking mitochondrial or cytosolic SODs that die around 21 days after birth or exhibit milder phenotypes, respectively, such as the development of cancer in time<sup>37</sup>. It appears if SOD levels and distributions are unchecked, this can contribute to mitochondrial damage and eventual cancer transformation<sup>16</sup>. Recent studies using both human and murine cancer models indicate that the expression of SOD2 is rapidly reduced upon activation of various oncogenes<sup>29</sup>, thus compromising its cytoprotective and antioxidative roles, presumably within the mitochondria. Thus, strategies to induce SOD2 may be an effective way to limit cancer transformation. On the other hand, SOD1 is overexpressed in a majority of mammary tumor models driven by various oncogenes<sup>29</sup>. It is possible that mitochondrial SOD1 may be necessary to maintain the integrity of the organelle when the levels of SOD2 are compromised during transformation. Indeed, after 10nM 1,25D<sub>3</sub> treatment for 48 hours there was a cumulative increase in the combined SOD1 and SOD2 transcript amounts compared to untreated MG-63 cells (**Figure 3F**). Nevertheless, the consensus is that in non-tumorigenic cells SOD2 levels are elevated while SOD1 levels are kept low<sup>29</sup>, suggesting that mitochondrial protection from ROS is critical in the natural high respiratory state. It was recently shown that pharmacological inhibition of SOD1 results in fragmented and dilated cristae of mitochondria in a breast cancer cell line (MDA-MB-231)<sup>29</sup>,



suggesting the critical role of SOD1 protection from mitochondrial ROS toxic effects during transformation. However, SOD1 inhibition within non-tumorigenic cells did not alter morphological features of the mitochondria<sup>29</sup>, presumably due to protection from the known increased endogenous levels of SOD2. These findings correlate with the long recognized understanding that cancer cells are characterized by elevated levels of ROS<sup>38</sup>. Furthermore, it has been reported that SIRT3 – a major regulator of SOD2 - expression is decreased in 87% of breast cancers implying a key role of SOD2 in cancer transformation<sup>39</sup>. Based on the findings presented here, vitamin D-mediate protection from ROS-induced damage can be attributed to the expression of the ROS detoxifier SOD2. Importantly, it appears that vitamin D has the potential to shift the SOD profile from one that represents a tumorigenic towards a non-tumorigenic state.

It is unclear how *SOD1* and *SOD2* expression is regulated by vitamin D and its receptor through *cis* and/or *trans* regulatory elements and factors. It is clear from the MTT data that other serum ligands work in synergy to support vitamin D's anti-cancer effects (**Figure 1A**), including the SOD1-to-SOD2 shift. It is possible that vitamin D regulates SOD1 and SOD2 expression via indirect mechanisms. For example, vitamin D is known to activate NRF2, which is a transcription factor that plays an important role in redox homeostasis and protection against oxidative damage<sup>40</sup>. Upon induction, NRF2 translocate to the nucleus and binds DNA antioxidant response elements (AREs) that leads to coordinated activation of gene expression<sup>41</sup>. Thus, vitamin D signaling may promote expression of NRF2 that then regulates antioxidant genes such as *SOD1* and *SOD2*, which remains to be tested<sup>41</sup>.

Previous studies using either *VDR* ablation or 1,25D<sub>3</sub> treatment approaches have made associations between *VDR* actions and mitochondrial respiratory activity along with production of intracellular ROS within several cell lines<sup>42</sup>. In all cell types it was found that upon *VDR* ablation there was an increase in respiration and ROS production associated with elevations in both mitochondrial COX2 and nuclear COX4I1<sup>42</sup>. On the other hand, 1,25D<sub>3</sub> treatment of skin keratinocytes resulted in decreased COX2 and COX4I1 mRNA levels, suggesting a concomitant reduction in intracellular ROS production<sup>36</sup>. Although in this study, evidence was provided for a mitochondrial-specific antioxidant effect of vitamin D within MG-63 cells, no change in either COX2 or COX4I1 transcript levels was found (**Figure 3A,B**). This would suggest that within MG-63 cells other vitamin D-dependent electron transport chain enzyme complexes may be involved, as ROS are sourced from Complex I and III enzymes, while Complex IV converts

molecular oxygen to two molecules of water and activates ATP synthase to synthesize ATP<sup>43</sup>. It is well-known that the maintenance of proper vitamin D levels for the long term will have beneficial cancer survival effects across demographics<sup>15</sup>, and in this paper, vitamin D was shown to significantly induce mitochondrial SOD2, and presume to be part of the antioxidant mechanism to limit the proliferation and cellular damage of MG-63 osteoblastoma cells. Future studies will focus on other non-calcemic vitamin D analogues and their effects on the SOD1-to-SOD2 switch and their role in cancer biology.

## **Experimental procedures**

### **Reagents and cell culture**

Crystalline 1,25(OH)<sub>2</sub>D<sub>3</sub> (Biomol, Plymouth Meeting, PA, USA) was reconstituted in ethanol and kept at -80°C. The vitamin D receptor antagonist ZK159222 (VAZ, Toronto Research Chemicals) was reconstituted in ethanol and kept at -80°C (Ochiai E et al. 2005).

Human MG-63 osteosarcoma cells (CRL-1427; American Type Culture Collection, Manassas, VA, USA) were cultured in complete media containing Eagle's Minimum Essential Medium (ATCC, 30-2003), 10% heat inactivated fetal bovine serum, and 1X penicillin and streptomycin. For some experiments, the cells were cultured in charcoal-stripped FBS (35-072-CV, Corning). For assays, cells were treated with 0 (vehicle) to 1 μM 1,25(OH)<sub>2</sub>D<sub>3</sub> incubated in tissue culture plates (CytoOne).

### **Quantitative real-time RT-PCR (qPCR) analyses**

RNA was prepared using the PureLink RNA Mini kit (ThermoFisher Scientific). cDNA was synthesized using 200 ng total RNA with the ProtoScript® First Strand cDNA Synthesis kit (New England Biolabs) utilizing random hexamers. All cDNAs were amplified under the following conditions: 95°C for 10 minutes to activate AmpliTaq Gold® Polymerase; followed by 40 cycles of 95°C for 15 seconds and 60°C for 1 minute with an internal ROX reference dye.

qPCR analysis was performed on a QuantStudio 3 Real-Time instrument (ThermoFisher Scientific) utilizing the Power SYBR™ Green PCR Master mix (ThermoFisher Scientific; primer list, Supplemental Table S1). Target genes were normalized to beta actin mRNA expression. For the primer design, the human genome sequence coverage assembly GRCh38.p13 was utilized from the Genome Reference Consortium.

### **MTT assay protocol for measuring cell viability**

All experiments were performed using 2.4×10<sup>4</sup> cells/well in 96-well plates. Cells were seeded and then left to incubate at 37°C (5%CO<sub>2</sub>) overnight. The following day, cells were carefully washed with 1X PBS, and then treated with 1,25D<sub>3</sub> and the cellular status was assessed at both 24 and 48 hours post treatment. The MTT (3-[4,5-dimethylthiazol-2-yl]-2,5 diphenyl tetrazolium bromide) assay was performed according to the manufacturer's recommendation (10009365, Cayman Chemicals). After incubation with the MTT reagent, the cells and salt were solubilized using the provided sodium dodecyl sulfate-based lysis buffer. The optical density absorbance

was determined using a Molecular Devices EMax microplate spectrophotometer at 550nm absorbance minus a 650nm reference. Data is represented as the mean of 5 replicate wells  $\pm$  SD, with analysis using the two-way ANOVA with Bonferroni post-hoc test (GraphPad Prism). In order to approximate the IC<sub>50</sub> value, GraphPad was used and applied nonlinear regression after log transformation of the 1,25D<sub>3</sub> dose assessed by the model:  $Y = \text{Bottom} + (\text{Top} - \text{Bottom}) / (1 + 10^{-(X - \text{LogIC}_{50})})$ .

### **Real-time PCR Data analysis**

Data are presented as fold induction of treatments compared to 0nM (vehicle) samples normalized to beta actin mRNA levels (i.e. the comparative CT Livak method (Livak, Schmittgen 2001)<sup>44</sup>. Melting curve analysis was performed for all primers to eliminate those that yielded primer-dimers. The *p*-values reflect the log fold-change compared to the vehicle (0nM) condition (*n*=3 experimental samples  $\pm$  SD). As the delta Ct (dCT) values are measures that are proportional to log expression, a t-test using two groups of dCT values was used to generate the *p*-values.

### **Competing interests**

The author has no competing interests to declare.

### **Author contributions**

T.S.L. designed and performed the experiments, analyzed the data, and wrote the manuscript.

### **Acknowledgement**

Supported by Grant # IRG-17-183-16 from the American Cancer Society, and from the Sylvester Comprehensive Cancer Center at the Miller School of Medicine, University of Miami

### **Data availability statement**

All data generated during and/or analyzed during the current study are available from the corresponding author on reasonable request.

## Main Figure Title and Legends

### Figure Legend

#### Figure 1.

**A) The impact of 1,25D<sub>3</sub> on MG-63 cell viability using the MTT assay.** The MTT assay was performed in experiments with complete serum or charcoal-stripped serum supplementation for 24 and 48 hours of incubation. The cells were treated with one addition of 1 pM to 1μM 1,25D<sub>3</sub> before the determination of cell viability.  $p \leq 0.05^*$ ,  $0.01^{**}$ ,  $0.001^{***}$  using the 2-way ANOVA with Bonferroni post hoc test ( $n=5$ ; error bars represent the SD).

**B) Logarithmic dose vs. response graph (MTT assay 24-48 hours).** The calculated  $\log IC_{50}$  for 1,25D<sub>3</sub> in 48 hours was 1.74 and the  $IC_{50}$  was 55.43nM. In this figure the Hill slope is 1.0, which describes the steepness of the curve. The value  $R^2$  (R square) quantifies goodness of fit. It is a fraction between 0.0 and 1.0 and has no units. Higher values indicate that the model fits the data better. In this graph, R square is 0.8773 and degree of freedom = 34.

**C) Degree of inhibition by 1,25D<sub>3</sub> on MG-63 osteosarcoma cells after 48 hours of treatment.** The maximal inhibition value was obtained with 1 μM 1,25D<sub>3</sub> and arbitrarily set to 100%.

**Figure 2.**

**A) PCNA transcript log-fold response.** Real-time PCR analysis of MG-63 cells in complete media.

**B) CYP24A1 transcript log-fold response.** Real-time PCR analysis of MG-63 cells in complete media.

**C) VDR transcript log-fold response.** Real-time PCR analysis of MG-63 cells in complete media.

**D) BGLAP transcript log-fold response.** Real-time PCR analysis of MG-63 cells in complete media.

$p \leq 0.05^*$ ,  $0.01^{**}$ ,  $0.001^{***}$  using the 2-way ANOVA with Bonferroni post hoc test (n=3; error bars represent the SD). VAZ (vitamin D receptor antagonist ZK159222)

**Figure 3.**

**A) COXII transcript log-fold response.** Real-time PCR analysis of MG-63 cells in complete media.

**B) COX4I1 transcript log-fold response.** Real-time PCR analysis of MG-63 cells in complete media.

**C) SOD1 transcript log-fold response.** Real-time PCR analysis of MG-63 cells in complete media.

**D) SOD2 transcript log-fold response.** Real-time PCR analysis of MG-63 cells in complete media.

**E) CAT transcript log-fold response.** Real-time PCR analysis of MG-63 cells in complete media.

**F) SOD1-to-SOD2 switch.** Transcript levels presented as arbitrary units normalized to beta actin amounts.

$p \leq 0.05^*$ ,  $0.01^{**}$ ,  $0.001^{***}$  using the 2-way ANOVA with Bonferroni post hoc test (n=3; error bars represent the SD). VAZ (vitamin D receptor antagonist ZK159222)

## Figure 4.

**Schema representing the SOD1-to-SOD2 switch in MG-63 osteosarcoma cells after vitamin D treatment.**

## Tables

Supplemental Table S1. Real-time PCR primer set (human)

Target Gene	Bp	Forward (5'-3')	Reverse (5'-3')	Reference
PCNA	180	TGTCGATAAAGAGGAGGAA GC	AAGTGTCCCATATCCGCAAT	CCDS13087
CYP24A1	188	TGGCTTCAGGAGAAGGAAA A	ACCAGGGTGCCTGAGTGTAG	NM_000782.5
VDR	192	GACCTCACCTCTGAGGACC A	GAACTTGATGAGGGGCTCAA	CCDS55820
BGLAP	202	GTGCAGAGTCCAGCAAAGG T	CGATAGGCCTCCTGAAAGC	NM_199173.6
CAT (catalase)	188	ATGTGCATGCAGGACAATCA	TCCTCATTGAGCACGTTAC	M3VXR8
SOD1	224	AGGCTGTACCAAGTGCAGGT C	CACCTTTGCCCAAGTCATCT	CCDS33536
SOD2	213	CTGGACAAACCTCAGCCCTA	CCTTGCAGTGGATCCTGATT	CCDS83141
ACTB	198	GCAAAGACCTGTACGCC AAC	ACATCTGCTGGAAGGTGGAC	NM_001101.5
COXIV	-	CGAGCAATTTCCACCTCT GT	GGTCAGCCGATCCATATAA	Consiglio M et al. 2015
COXII	-	CGACTACGGCGGACTAA TCT	TCGATTGTCAACGTCAAGGA	Consiglio M et al. 2015

## References

- 1 Tian, X. Q., Chen, T. C., Matsuoka, L. Y., Wortsman, J. & Holick, M. F. Kinetic and thermodynamic studies of the conversion of previtamin D3 to vitamin D3 in human skin. *The Journal of biological chemistry* **268**, 14888-14892 (1993).
- 2 Lagishetty, V. *et al.* Vitamin D deficiency in mice impairs colonic antibacterial activity and predisposes to colitis. *Endocrinology* **151**, 2423-2432, doi:10.1210/en.2010-0089 (2010).
- 3 Lisse, T. S., Adams, J. S. & Hewison, M. Vitamin D and microRNAs in bone. *Critical reviews in eukaryotic gene expression* **23**, 195-214 (2013).
- 4 Lisse, T. S., Chun, R. F., Rieger, S., Adams, J. S. & Hewison, M. Vitamin D activation of functionally distinct regulatory miRNAs in primary human osteoblasts. *Journal of bone and mineral research : the official journal of the American Society for Bone and Mineral Research* **28**, 1478-1488, doi:10.1002/jbmr.1882 (2013).
- 5 Lisse, T. S. & Hewison, M. Vitamin D: a new player in the world of mTOR signaling. *Cell cycle* **10**, 1888-1889 (2011).
- 6 Lisse, T. S., Hewison, M. & Adams, J. S. Hormone response element binding proteins: novel regulators of vitamin D and estrogen signaling. *Steroids* **76**, 331-339, doi:10.1016/j.steroids.2011.01.002 (2011).
- 7 Lisse, T. S. *et al.* Gene targeting by the vitamin D response element binding protein reveals a role for vitamin D in osteoblast mTOR signaling. *FASEB journal : official publication of the Federation of American Societies for Experimental Biology* **25**, 937-947, doi:10.1096/fj.10-172577 (2011).
- 8 Lisse, T. S. *et al.* The vitamin D receptor is required for activation of cWnt and hedgehog signaling in keratinocytes. *Molecular endocrinology* **28**, 1698-1706, doi:10.1210/me.2014-1043 (2014).
- 9 Lisse, T. S. *et al.* The heterodimeric structure of heterogeneous nuclear ribonucleoprotein C1/C2 dictates 1,25-dihydroxyvitamin D-directed transcriptional events in osteoblasts. *Bone research* **2**, doi:10.1038/boneres.2014.11 (2014).
- 10 Zhang, X. *et al.* DNA damage-inducible transcript 4 is an innate guardian for human squamous cell carcinoma and an molecular vector for anti-carcinoma effect of 1,25(OH)<sub>2</sub> D<sub>3</sub>. *Experimental dermatology* **28**, 45-52, doi:10.1111/exd.13815 (2019).
- 11 Zhao, H., Rieger, S., Abe, K., Hewison, M. & Lisse, T. S. DNA Damage-Inducible Transcript 4 Is an Innate Surveillant of Hair Follicular Stress in Vitamin D Receptor Knockout Mice and a Regulator of Wound Re-Epithelialization. *International journal of molecular sciences* **17**, doi:10.3390/ijms17121984 (2016).
- 12 Zhou, R. *et al.* Vitamin D and alternative splicing of RNA. *The Journal of steroid biochemistry and molecular biology* **148**, 310-317, doi:10.1016/j.jsbmb.2014.09.025 (2015).
- 13 Zhou, R. *et al.* Concerted effects of heterogeneous nuclear ribonucleoprotein C1/C2 to control vitamin D-directed gene transcription and RNA splicing in human bone cells. *Nucleic acids research* **45**, 606-618, doi:10.1093/nar/gkw851 (2017).
- 14 Bouillon, R. *et al.* Vitamin D and human health: lessons from vitamin D receptor null mice. *Endocrine reviews* **29**, 726-776, doi:10.1210/er.2008-0004 (2008).
- 15 Manson, J. E. *et al.* Vitamin D Supplements and Prevention of Cancer and Cardiovascular Disease. *The New England journal of medicine* **380**, 33-44, doi:10.1056/NEJMoa1809944 (2019).
- 16 Sheng, Y. *et al.* Superoxide dismutases and superoxide reductases. *Chemical reviews* **114**, 3854-3918, doi:10.1021/cr4005296 (2014).
- 17 Berridge, M. J. Vitamin D, reactive oxygen species and calcium signalling in ageing and disease. *Philos Trans R Soc Lond B Biol Sci* **371**, doi:10.1098/rstb.2015.0434 (2016).
- 18 Wang, Y., Branicky, R., Noe, A. & Hekimi, S. Superoxide dismutases: Dual roles in controlling ROS damage and regulating ROS signaling. *The Journal of cell biology* **217**, 1915-1928, doi:10.1083/jcb.201708007 (2018).



- 19 Lisse, T. S. & Rieger, S. IKKalpha regulates human keratinocyte migration by surveillance of the redox environment. *Journal of cell science*, doi:10.1242/jcs.197343 (2017).
- 20 Tao, R. *et al.* Sirt3-mediated deacetylation of evolutionarily conserved lysine 122 regulates MnSOD activity in response to stress. *Molecular cell* **40**, 893-904, doi:10.1016/j.molcel.2010.12.013 (2010).
- 21 Liu, X. *et al.* Sirt3-dependent deacetylation of SOD2 plays a protective role against oxidative stress in oocytes from diabetic mice. *Cell cycle* **16**, 1302-1308, doi:10.1080/15384101.2017.1320004 (2017).
- 22 Zenmyo, M. *et al.* Transcriptional activation of p21 by vitamin D(3) or vitamin K(2) leads to differentiation of p53-deficient MG-63 osteosarcoma cells. *Hum Pathol* **32**, 410-416, doi:10.1053/hupa.2001.23524 (2001).
- 23 Ryhanen, S., Jaaskelainen, T., Mahonen, A. & Maenpaa, P. H. Inhibition of MG-63 cell cycle progression by synthetic vitamin D3 analogs mediated by p27, Cdk2, cyclin E, and the retinoblastoma protein. *Biochem Pharmacol* **66**, 495-504, doi:10.1016/s0006-2952(03)00283-1 (2003).
- 24 Vishlaghi, N. & Lisse, T. S. Exploring vitamin D signalling within skin cancer. *Clinical endocrinology*, doi:10.1111/cen.14150 (2019).
- 25 Shimizu, T. *et al.* Calcitriol exerts an anti-tumor effect in osteosarcoma by inducing the endoplasmic reticulum stress response. *Cancer science* **108**, 1793-1802, doi:10.1111/cas.13304 (2017).
- 26 Peehl, D. M. *et al.* Molecular activity of 1,25-dihydroxyvitamin D3 in primary cultures of human prostatic epithelial cells revealed by cDNA microarray analysis. *The Journal of steroid biochemistry and molecular biology* **92**, 131-141, doi:10.1016/j.jsbmb.2004.07.003 (2004).
- 27 Lambert, J. R. *et al.* Prostate derived factor in human prostate cancer cells: gene induction by vitamin D via a p53-dependent mechanism and inhibition of prostate cancer cell growth. *Journal of cellular physiology* **208**, 566-574, doi:10.1002/jcp.20692 (2006).
- 28 Bao, B. Y., Ting, H. J., Hsu, J. W. & Lee, Y. F. Protective role of 1 alpha, 25-dihydroxyvitamin D3 against oxidative stress in nonmalignant human prostate epithelial cells. *International journal of cancer* **122**, 2699-2706, doi:10.1002/ijc.23460 (2008).
- 29 Papa, L., Hahn, M., Marsh, E. L., Evans, B. S. & Germain, D. SOD2 to SOD1 switch in breast cancer. *The Journal of biological chemistry* **289**, 5412-5416, doi:10.1074/jbc.C113.526475 (2014).
- 30 Muindi, J. R., Modzelewski, R. A., Peng, Y., Trump, D. L. & Johnson, C. S. Pharmacokinetics of 1alpha,25-dihydroxyvitamin D3 in normal mice after systemic exposure to effective and safe antitumor doses. *Oncology* **66**, 62-66, doi:10.1159/000076336 (2004).
- 31 Mizwicki, M. T. *et al.* On the mechanism underlying (23S)-25-dehydro-1alpha(OH)-vitamin D3-26,23-lactone antagonism of hVDRwt gene activation and its switch to a superagonist. *The Journal of biological chemistry* **284**, 36292-36301, doi:10.1074/jbc.M109.042069 (2009).
- 32 Parise, R. A. *et al.* CYP24, the enzyme that catabolizes the antiproliferative agent vitamin D, is increased in lung cancer. *International journal of cancer* **119**, 1819-1828, doi:10.1002/ijc.22058 (2006).
- 33 Sergeev, I. N. Vitamin D-mediated apoptosis in cancer and obesity. *Horm Mol Biol Clin Investig* **20**, 43-49, doi:10.1515/hmbci-2014-0035 (2014).
- 34 Patti, A., Gennari, L., Merlotti, D., Dotta, F. & Nuti, R. Endocrine actions of osteocalcin. *International journal of endocrinology* **2013**, 846480, doi:10.1155/2013/846480 (2013).
- 35 Gao, J. *et al.* SIRT3/SOD2 maintains osteoblast differentiation and bone formation by regulating mitochondrial stress. *Cell Death Differ* **25**, 229-240, doi:10.1038/cdd.2017.144 (2018).

- 36 Consiglio, M. *et al.* Mitochondrial and lipogenic effects of vitamin D on differentiating and proliferating human keratinocytes. *Experimental dermatology* **24**, 748-753, doi:10.1111/exd.12761 (2015).
- 37 Sentman, M. L. *et al.* Phenotypes of mice lacking extracellular superoxide dismutase and copper- and zinc-containing superoxide dismutase. *The Journal of biological chemistry* **281**, 6904-6909, doi:10.1074/jbc.M510764200 (2006).
- 38 Lu, W., Ogasawara, M. A. & Huang, P. Models of reactive oxygen species in cancer. *Drug Discov Today Dis Models* **4**, 67-73, doi:10.1016/j.ddmod.2007.10.005 (2007).
- 39 Finley, L. W. *et al.* SIRT3 opposes reprogramming of cancer cell metabolism through HIF1alpha destabilization. *Cancer cell* **19**, 416-428, doi:10.1016/j.ccr.2011.02.014 (2011).
- 40 Nakai, K. *et al.* Vitamin D activates the Nrf2-Keap1 antioxidant pathway and ameliorates nephropathy in diabetic rats. *Am J Hypertens* **27**, 586-595, doi:10.1093/ajh/hpt160 (2014).
- 41 Lisse, T. S., King, B. L. & Rieger, S. Comparative transcriptomic profiling of hydrogen peroxide signaling networks in zebrafish and human keratinocytes: Implications toward conservation, migration and wound healing. *Scientific reports* **6**, 20328, doi:10.1038/srep20328 (2016).
- 42 Ricca, C. *et al.* Vitamin D Receptor Is Necessary for Mitochondrial Function and Cell Health. *International journal of molecular sciences* **19**, doi:10.3390/ijms19061672 (2018).
- 43 Murphy, M. P. How mitochondria produce reactive oxygen species. *Biochem J* **417**, 1-13, doi:10.1042/BJ20081386 (2009).
- 44 Livak, K. J. & Schmittgen, T. D. Analysis of relative gene expression data using real-time quantitative PCR and the 2(-Delta Delta C(T)) Method. *Methods* **25**, 402-408, doi:10.1006/meth.2001.1262 (2001).

## Figures

Figure 1.

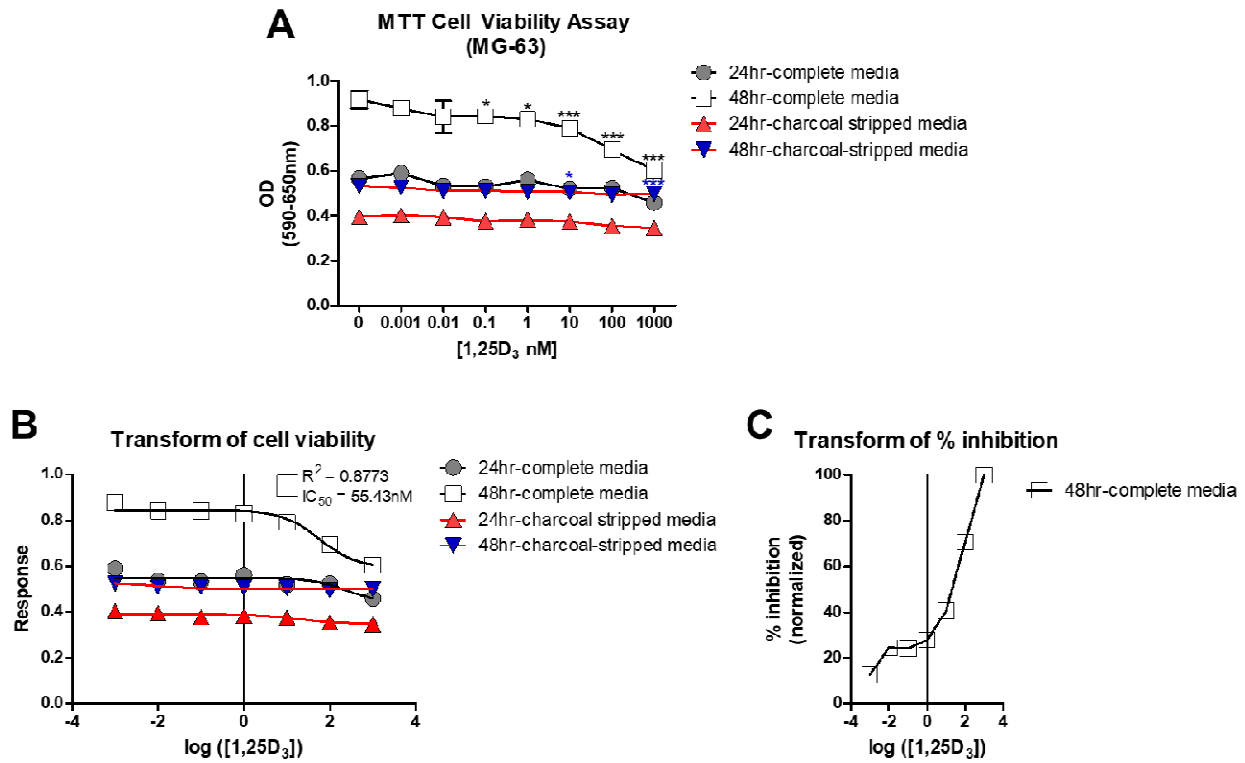


Figure 2.

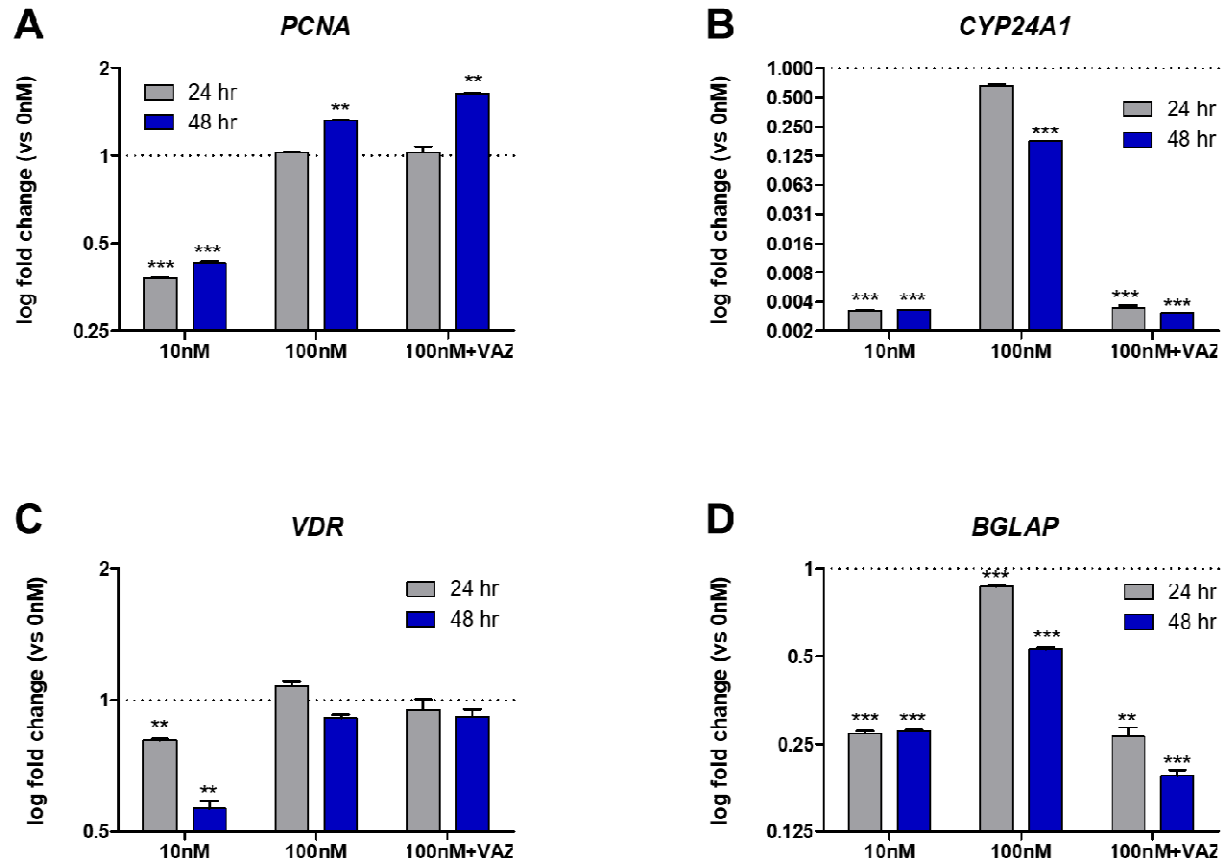


Figure 3.

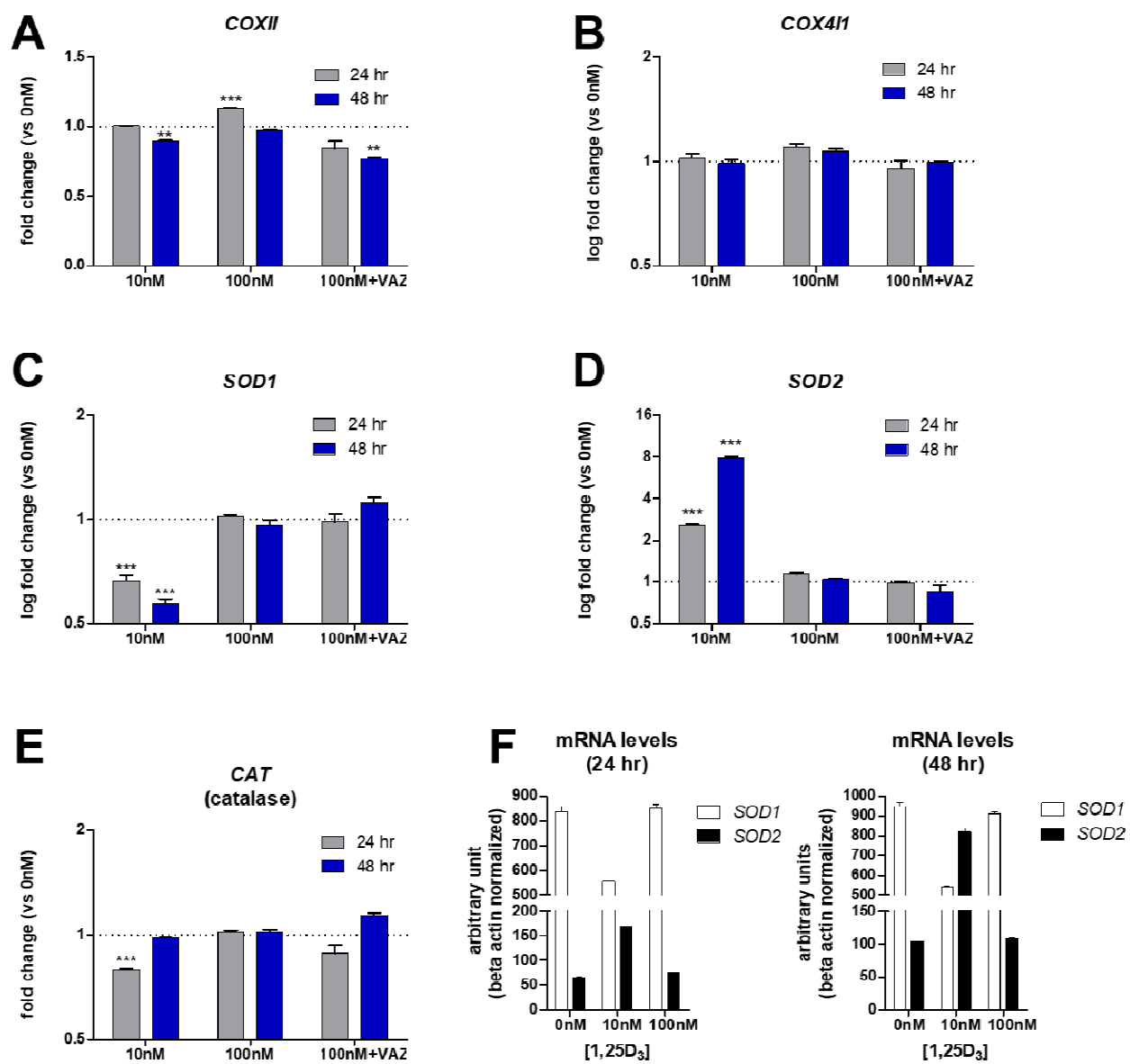
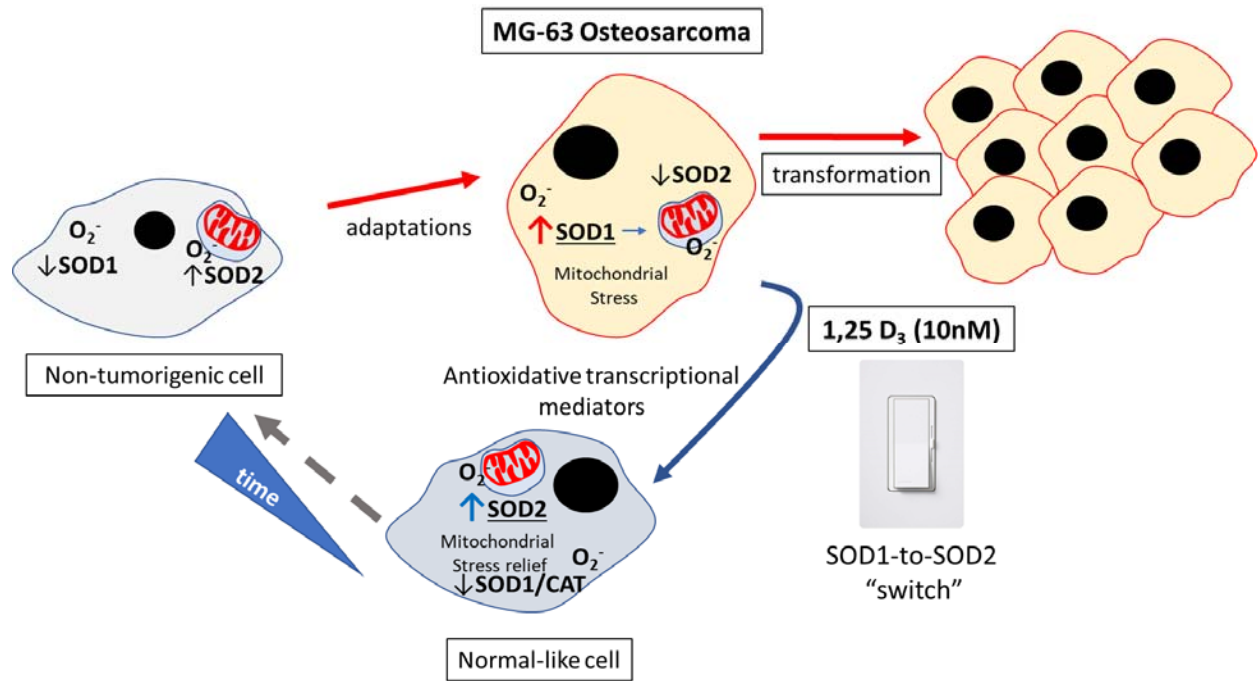
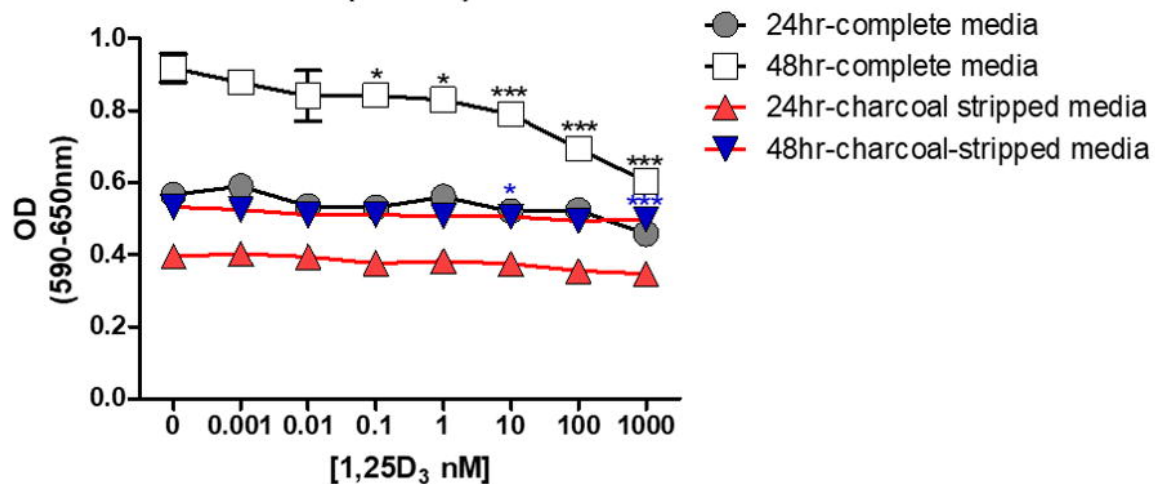


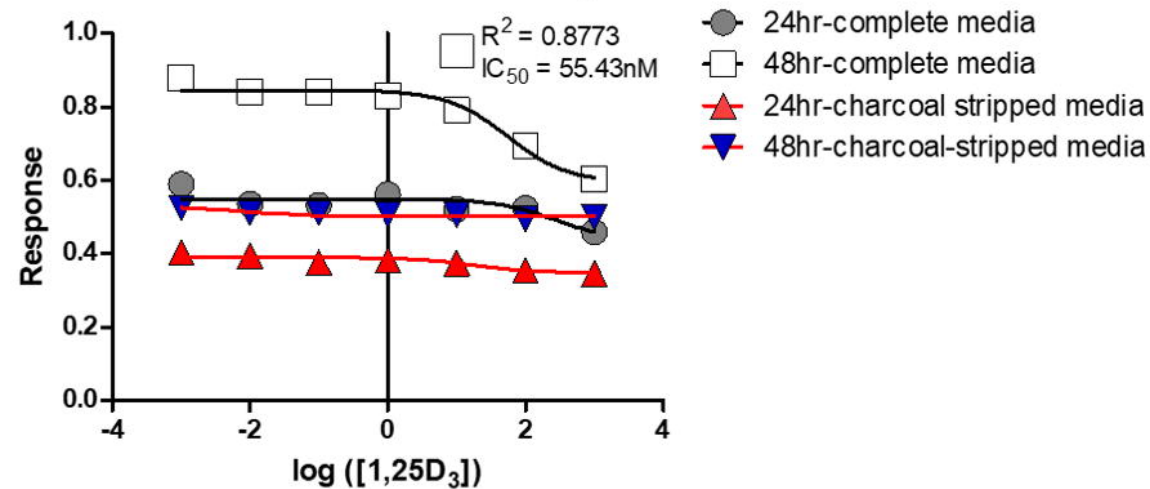
Figure 4.



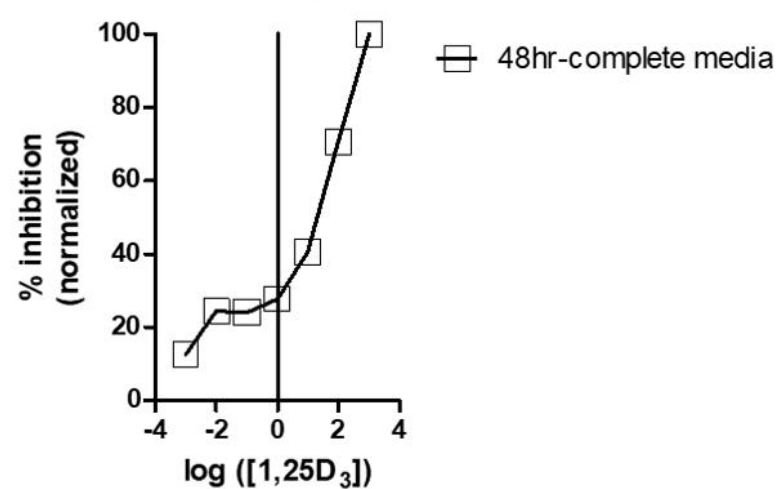
### A MTT Cell Viability Assay (MG-63)

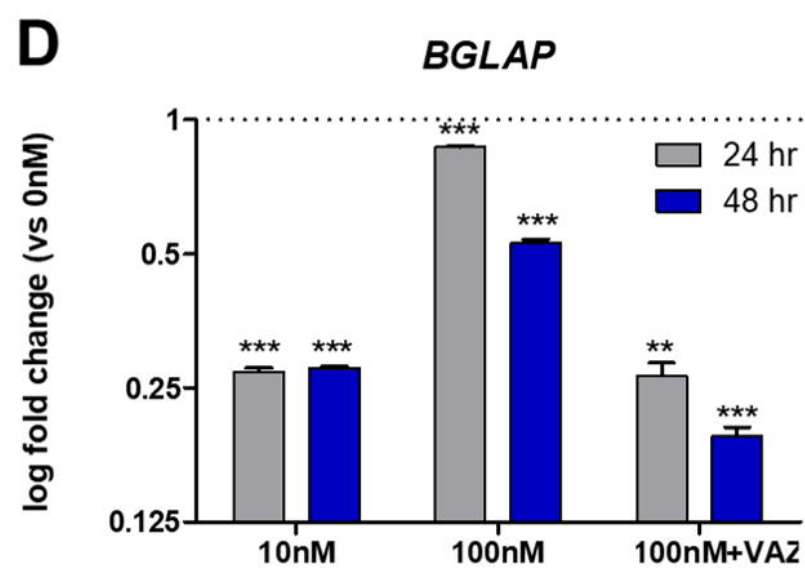
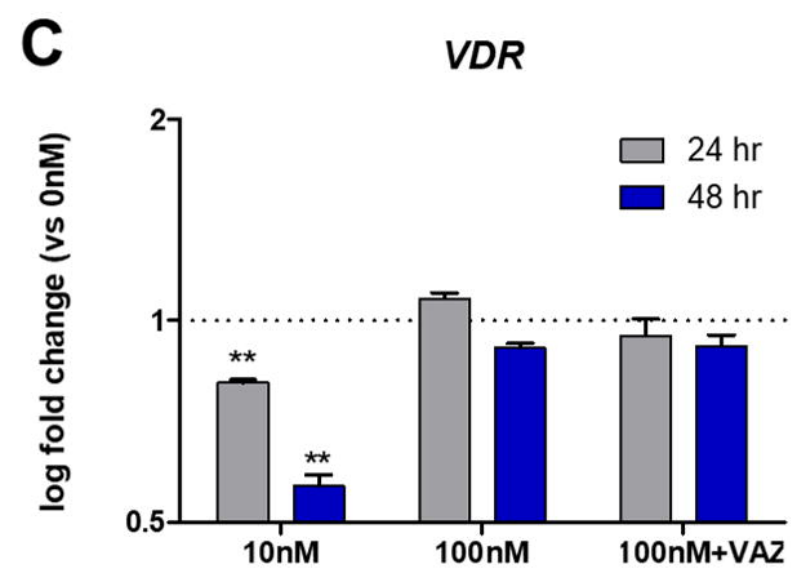
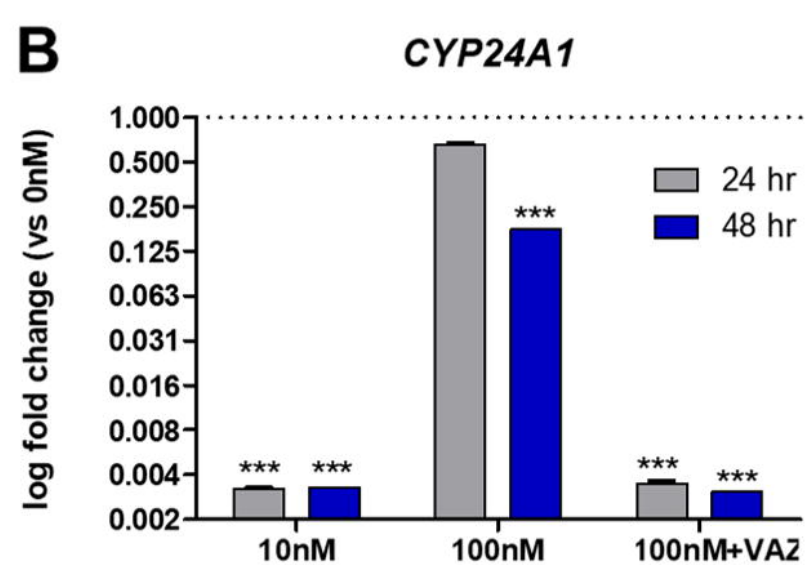
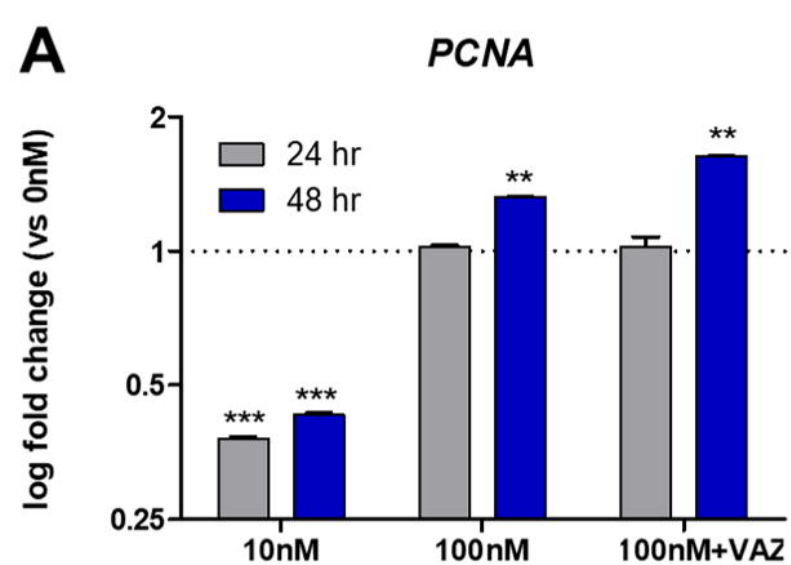


### B Transform of cell viability

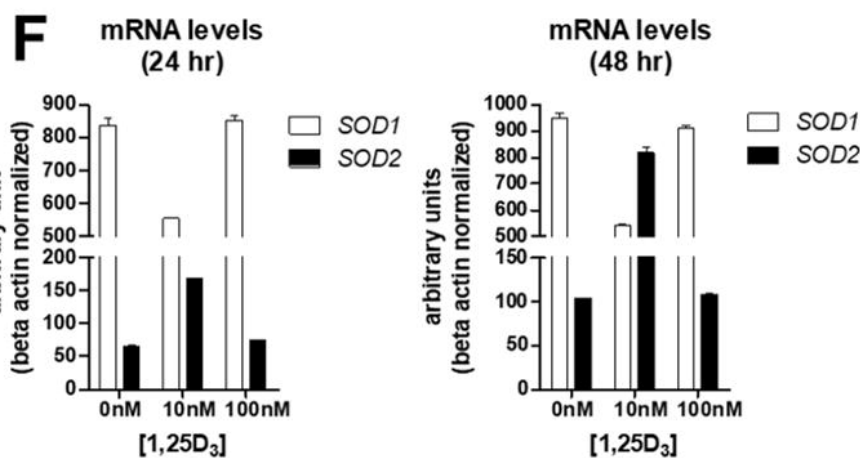
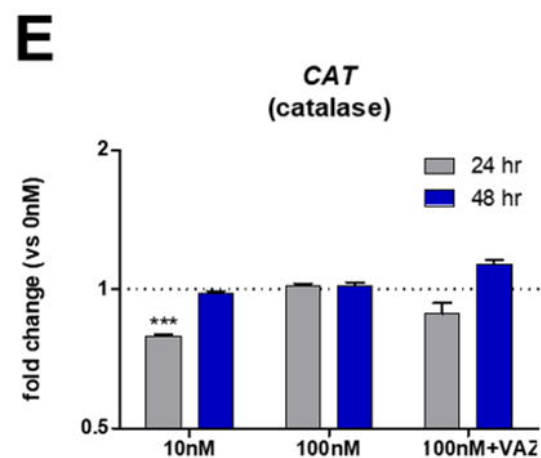
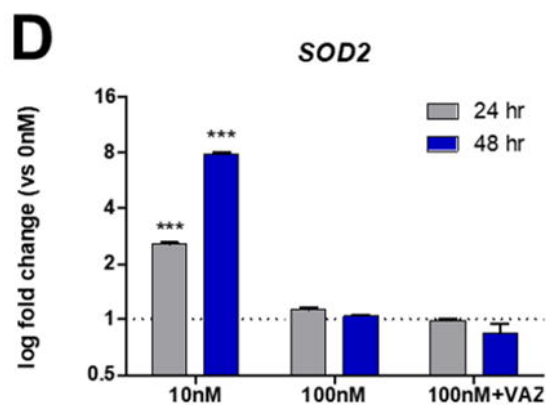
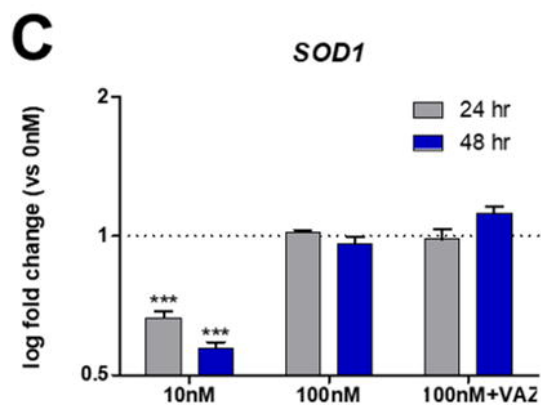
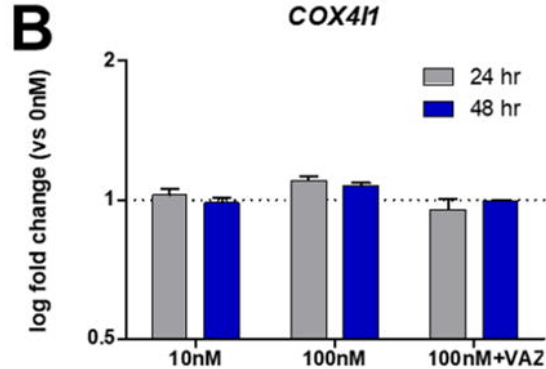
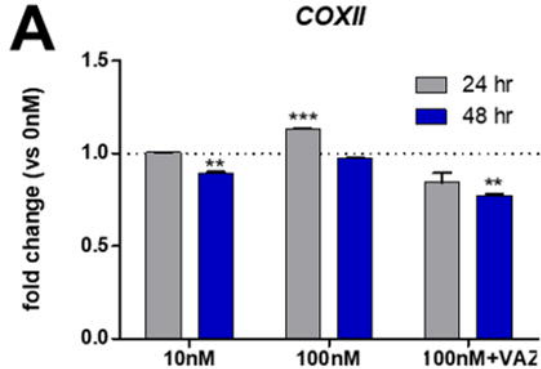


### C Transform of % inhibition

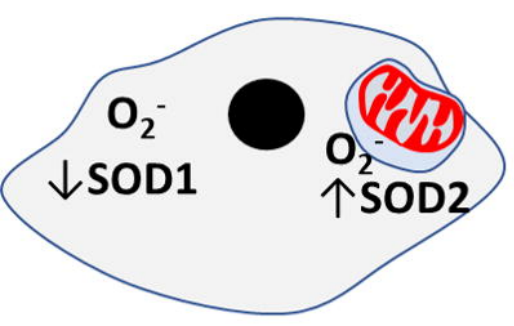






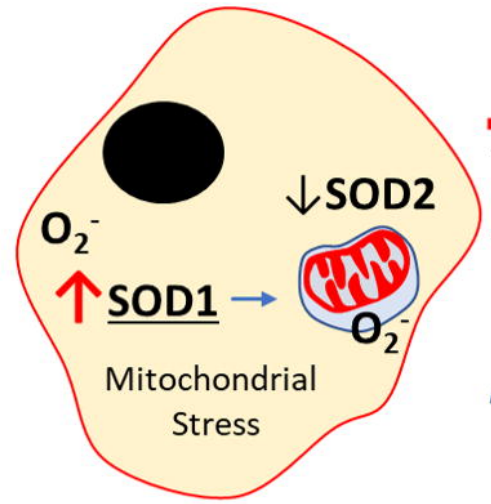


# MG-63 Osteosarcoma

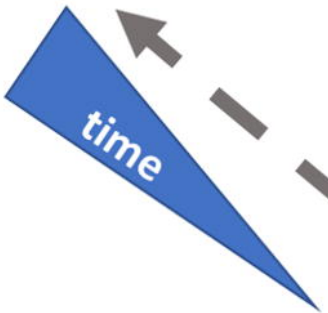
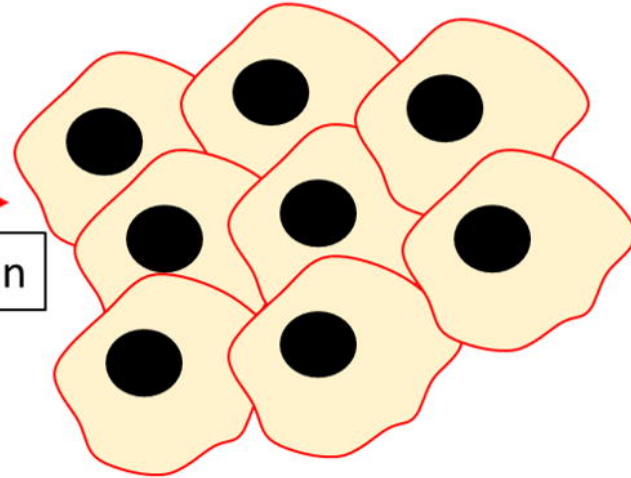


Non-tumorigenic cell

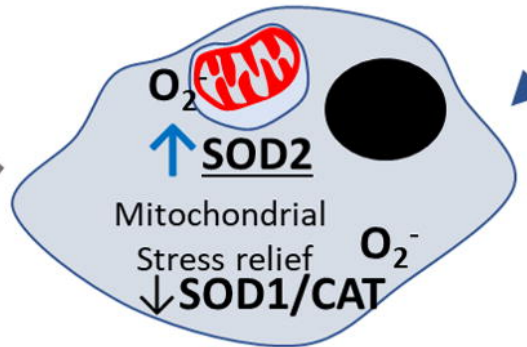
adaptations



transformation



Antioxidative transcriptional mediators



Normal-like cell

1,25 D<sub>3</sub> (10nM)



SOD1-to-SOD2 "switch"